ECOPERSIA

DOI:10.18869/modares.Ecopersia.4.4.1527 **2016, 4 (4): 1527-1540**

Relative Humidity and Moisture Flux Convergence during the Dusty Days in Alvand Mountain

Deeman Ghaffari[1] and Hamid Nouri[2]

[1] *Former Master Student of Watershed Management, Department of Rangeland and Watershed Management, Malayer University, Malayer, Iran*
[2] *Assistant Professor of Climatology, Department of Rangeland and Watershed Management Malayer University, Malayer, Iran*

Received: 7 November 2015 / Accepted: 11 July 2016 / Published Online: 9 December 2016

ABSTRACT The moisture flux convergence (MFC) and relative humidity in dusty days at different times and levels over the Alvand Mountain was investigated. The required basic data for the years 2009-2012, including relative humidity, visibility and synoptic codes, were gathered from Hamadan synoptic station, while sea level pressure, uwind, vwind and specific humidity data were gathered from NCER/NCAR site. The dusty days were categorized into four groups, according to WMO protocol. Sea level pressure (SLP) patterns were classified using cluster analysis (CA). MFC function, jet stream and omega maps were computed using special moisture and horizontal and vertical components of wind, SLP and omega data in various levels and times for each sea level pressure pattern. The results showed 6 categorized patterns of sea level pressure. The highest values of MFC were observed at 1000, 925 and 850 hPa levels and at 12:00 and 18:00 UTC. MFC value strongly decreased in dusty days at the 700, 600 and 500 hPa and at 06:00 UTC. The relative humidity significantly decreased at 12:00, while the maximum increase was recorded at 18:00 and 00:00 UTC.

Key words: *Sea level pressure (SLP), Omega, Temporal variations, Dust storms, Hamadan*

1 INTRODUCTION

In the recent years, movement of dust from Jordan, Syria, Iraq and North of Arabian Peninsula toward the west and southwest of Iran has been a common phenomenon in the warm seasons (Azizi *et al*., 2012). The height and expanse of dust in the atmosphere depends on wind speed, humidity and size of the particles. Intensity and expanse of dust may be a reaction to vegetation cover and humidity in the soil and atmosphere Dust storms have a negative effect on Tourism. Dust causes' disorder in photosynthesis and dryness in branches of trees and plants. The development and improvement of local and temporal analysis techniques is used for forecasting the primary amounts of convective in short time (3 hours) and their spatial variations. According to the literature, MFC can be used to estimate large scale rains, forecasting the place of primary convective, forecasting the convective clouds covers. Several researches were conducted to investigate the intensity, extension, eradicating and the way of dust transportation in various regions of the

**Corresponding author: Former Master Student of Watershed Management, Department of Rangeland and Watershed Management, Malayer University, Malayer, Iran, Tel: +98 918 612 5882, E-mail: Di3000gh@yahoo.com.*

world. Banacos and Schultz (2005) used MFC to forecast the convective rains. They showed extensive effect of MFC on boundary layers between different air bulks. They concluded that the surface MFC was related to horizontal convergence. Omidvar (2006) introduced the dynamic low-pressure and cold front as the main factor of dust formation in the Yazd-Ardakan Plain. Karimi-Ahmadabad and Farajzadeh-Asl (2009) stated that moisture resources of Iran with different MFC in various levels of atmosphere are due to steam aggregation by horizontal advection to various layers of atmosphere. Farajzadeh-Asl *et al.* (2007) showed that Oman Sea and Arabian Sea are the most basic source of moisture in west of Iran. In this regard, transmission of cold air on the region with intense temperature gradient and surface pressure has provided astatic erect air flows for emersion of dust storms. Saavedra *et al.* (2010) defined the relevance of synoptic patterns in transportation of ozone air bulk in northwest Spain and showed that ozone transportation was more frequent in Portugal and Mediterranean due to blocking establishment. The relationships of MFC and extreme rain in Chabahar coats was attributed to the Adan Gulf and southwestern convergence in the Red Sea (Ghavidel- Rahimi, 2011). Frequency analysis of Asian dust storms by Lee and Kim (2012) showed that strong winds, shortage of plants coverage and snow were the main reasons of dust events. Csavina *et al.* (2014) reported that wind speed and relative humidity accelerated the density of dusts, which increased to maximum rate at 25% of relative humidity, above which the dusts density decreased. Synoptic analysis of dust phenomenon in Mashhad (1980-2009) showed that most of the storms occurred in summer season (Mosavi and Ashraf, 2012). The frequency of MFC in the extreme rain events (convective and non-convective) of south coasts of the Caspian identified various moisture source (Nouri *et al.*, 2013); the highest values of MFC rates occurred at 06:00. Also, the extreme rain group with convective origin had a higher value relative to other groups. Despite various works in this area, studies on atmospheric thickness, jet stream of moisture, and MFC rate in various levels and occurrence time and its effect on dust storm formation are limited.

Hamadan province is one of the regions that faces with dust storm and is under influence of this destructive phenomenon. Defining the air pressure patterns, MFC and relative humidity during the dusty days in Hamadan is the main aim of this study, which can be an important step in recognition of dynamic and thermodynamic conditions of atmosphere during the occurrence of dust storms at different times and levels over the Alvand mountain.

2 MATERIALS AND METHODS

The Zagros mountain range has a total length of 1500 km that begins in northwest and ends at the Strait of Hormuz. The annual precipitation range is 400 to 800 mm that pours mostly in winter and spring. Alvand is a mountain in the Zagros range in western Iran, 34°N to 48°E, located 10 km south of Hamedan city, with an elevation of 3580 meters.

The required data for MFC and relative humidity during the dusty days were provided by the Hamadan synoptic station from 2009 to 2012. The sea levels pressure (SLP), uwind (the positive u wind is from the west, while the negative u wind is from the east), vwind (the positive v wind is from the south while the negative v wind is from the north), and specific humidity data were obtained from NCER/NCAR site (http://www.esrl.noaa.gov/).

Based on visibility (VV) and synoptic cods (WW) of the WMO protocol (UN Environment Program, 2013), the observed dusty days over the Alvand Mountain (provided by Hamadan

[DOR: 20.1001.1.23222700.2016.4.4.6.3]

synoptic station) were categorized into four groups (DIS, BD, DS and SDS) (Table1).

Table 1 Dust event categories based on visibility (VV) and synoptic cods (WW)

Dust event categories	WW	VV	
DIS_1	05	10000 m	DIS
DIS_2	06		
DIS_3	07		
DIS_4	08		
BD_1	05	1000 – 10000 m	BD
BD_2	06		
BD_3	07		
BD_4	08		
BD_5	09		
DS_1	06	200 – 1000 m	DS
DS_2	07		
DS_3	08		
DS_4	09		
DS_5	30		
DS_6	31		
DS_7	32		
SDS_1	32	Less than 200 m	SDS
SDS_2	33		
SDS_3	34		
SDS_4	35		

Maps of sea level pressure (SLP) on daily mean and 6 hour interval basis were used. This corresponded to data of the NCEP Reanalysis 2 that represent atmospheric circulation at low levels, which is highly important in determining moisture advection (Penalba and Bettolli, 2010). The study was conducted for the period of 2009-2012 at a domain from 0°N to 80°N and from 0°E to 120° E., which extends over the Asia and Europe that significantly influence the atmospheric circulation over the Alvand Mountain. The data was set in S-shape. The rows in the matrix represented time, while columns represented space. Based on Ward Linkage method, a hierarchical cluster analysis was conducted on the Euclidean distance set. The 6 hours maps and mean daily maps of sea level pressure were identified using MATLAB software and the synoptic patterns computed were mapped by GRADS software. Meanwhile, the subjective method was used to determine the number of patterns. In this study, the influence of atmospheric MFC and the relative humidity on dust was investigated, with a focus on the Alvand Mountain.

Thus, MFC in each sea level pressure (SLP) during the dusty days was studied. MFC is a term used in calculation of predicting rainfall (Banacos and Schultz, 2005), and can be calculated by the following equations (Eq. 1, 2).

$$MFC = -\nabla \cdot (q\vec{V}_h) = -\vec{V}_h \cdot \nabla q - q\nabla \cdot \vec{V}_h, \quad (1)$$

MFC = convergence term – advection term (2)

The advection term represents the horizontal advection of specific humidity. The convergence term denotes the product of the specific humidity and horizontal mass convergence. Where q is specific humidity and V is horizontal velocity. Vertically integrated MFC is equivalent in the long term mean to net

[DOR: 20.1001.1.23222700.2016.4.4.6.3]

precipitation (P-E), and in turn to river runoff. MFC value were estimated from the vertically-integrated moisture fluxes, which were calculated based on the 6-hourly wind velocity (uwind and vwind) and specific humidity (q) at all vertical levels (925, 850, 700, 600, 500, 400, 300, 200 and 100 hPa), and surface level pressure (1000 hPa) for each 6 hour interval (00:00, 06:00, 12:00 and 18:00 UTC) during the dusty days and for each SLP patterns.

The representative days for SLP patterns are computed based on maximum correlation coefficient in the groups. SLP patterns, MFC, jet stream and omega maps in different levels and in dust days over the Alvand Mountain were analyzed for representative days.

3 RESULTS

The dust events were observed all the year, especially from April to July over the Alvand Mountain. BD_2 was the most frequent dust group with its origin out of station (Figure 1). Table (2) indicates sea level pressure patterns (6 patterns) and their representative day in dusty days in the Alvand Mountain. Figures 2 to 25 show SLP patterns, MFC (1000 hPa), jet stream (300 hPa) and omega (1000 hPa) maps in dusty days over the Alvand Mountain.

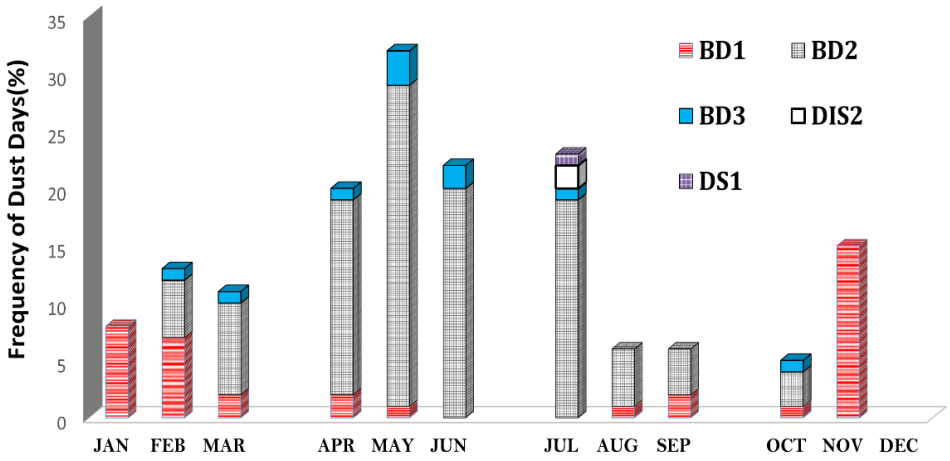

Figure 1 Monthly distribution of the dust categories in the Alvand Mountain (2009-2012)

Table 2 Sea level pressure patterns and their representative day.

Correlation of representative day and group data %	Representative day	Sea level pressure
62	21 Dec 2010	North Caspian Sea high pressure: SLP pattern 1
87	19 Jan 2011	Eurasia combined high pressure-Polar and equator twine low pressure: SLP pattern 2
50	14 Jan 2011	East Caspian Sea twine high pressure and African high pressure: SLP pattern 3
48	25 Jun 2010	Iranian mountainous area low pressure: SLP pattern 4
99	29 Sep 2010	Torkamanestan high pressure and Arabestan low pressure: SLP pattern 5

[DOR: 20.1001.1.23222700.2016.4.4.6.3]

99	13 May 2010	Eurasia high pressure and Iraq low pressure: SLP pattern 6

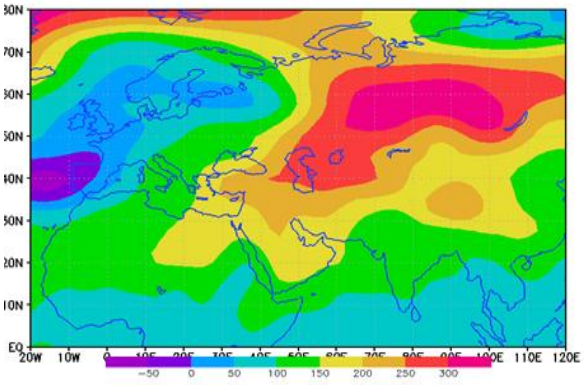

Figure 2 SLP pattern1 map in dusty days

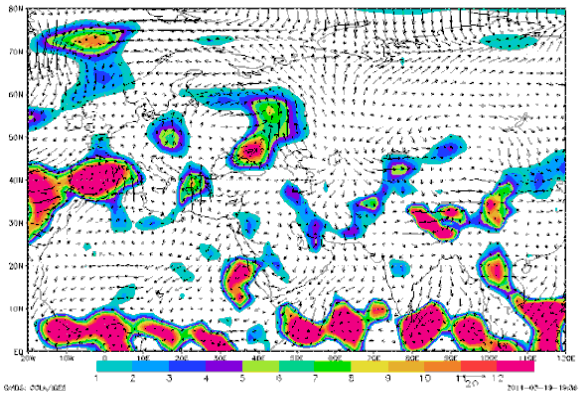

Figure 3 MFC map (1000 hPa) in SLP pattern 1 in dusty days

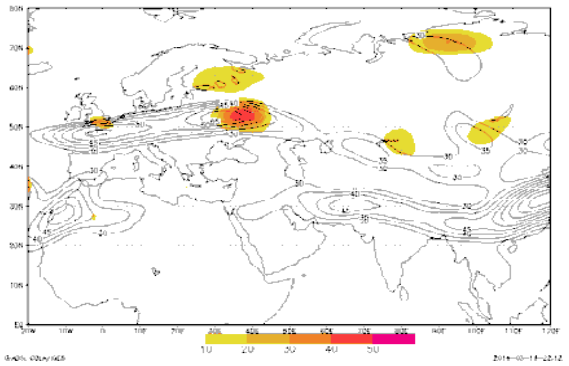

Figure 4 Jet stream map (300 hPa) in SLP pattern 1 in dusty days

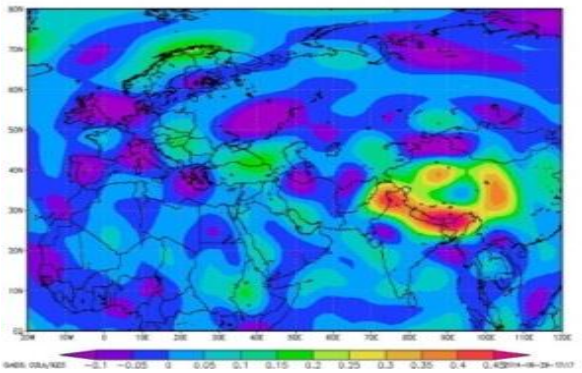

Figure 5 Omega map (1000 hPa) in SLP pattern 1 in dusty days

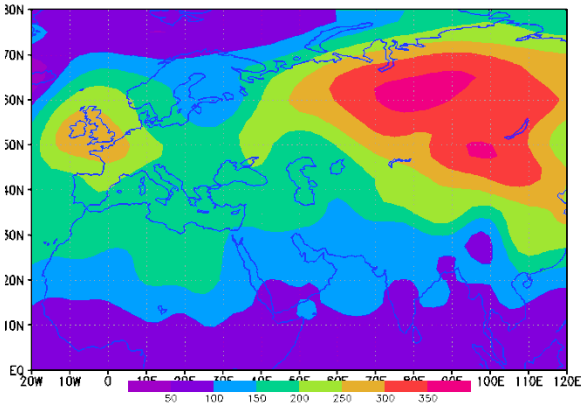

Figure 6 SLP pattern 2 map in dusty days

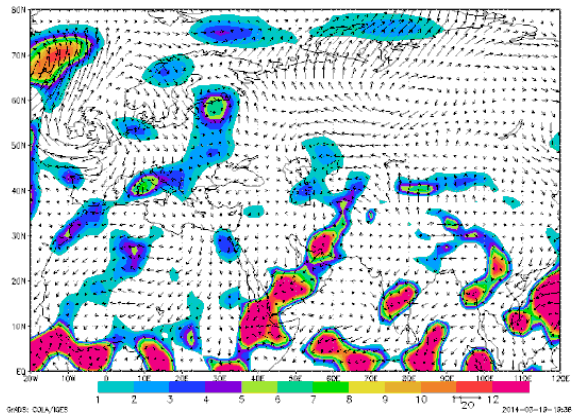

Figure 7 MFC map (1000 hPa) in SLP pattern 2 in

[DOR: 20.1001.1.23222700.2016.4.4.6.3]

dusty days

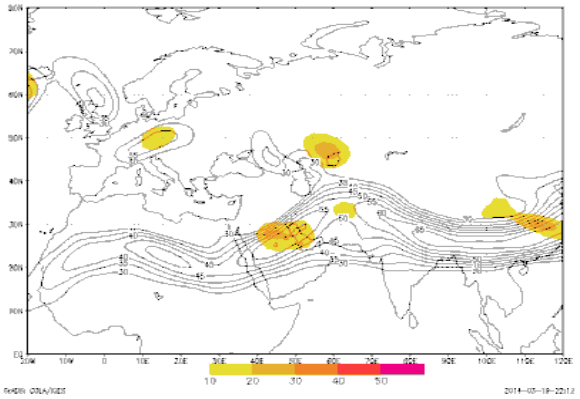

Figure 8 Jet stream map (300 hPa) in SLP pattern 2 in dusty days

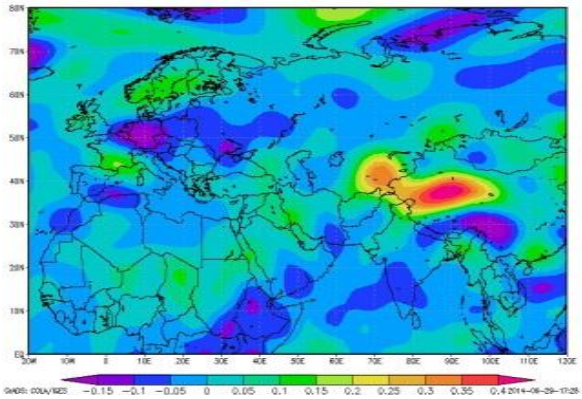

Figure 9 Omega map (1000 hPa) in SLP pattern 2 in dusty days

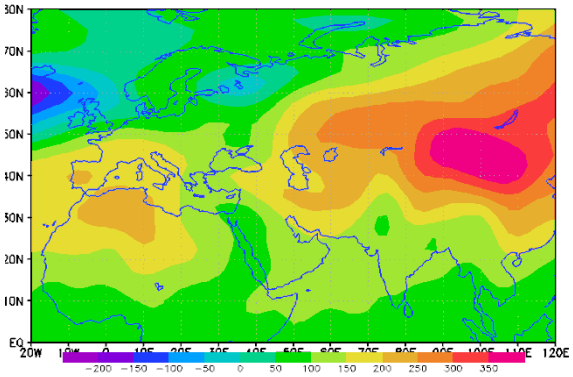

Figure 10 SLP pattern 3 map in dusty days

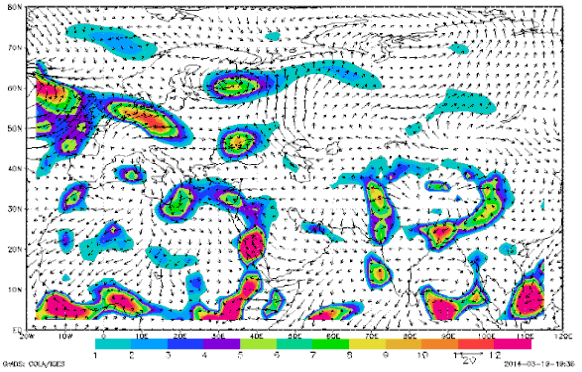

Figure 11 MFC map (1000 hPa) in SLP pattern 3 in dusty days

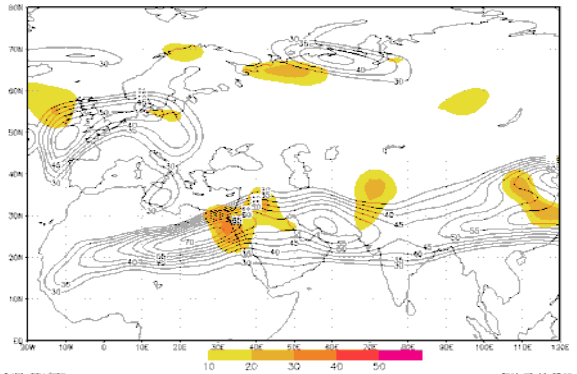

Figure 12 Jet stream map (300 hPa) in SLP pattern 3 in dusty days

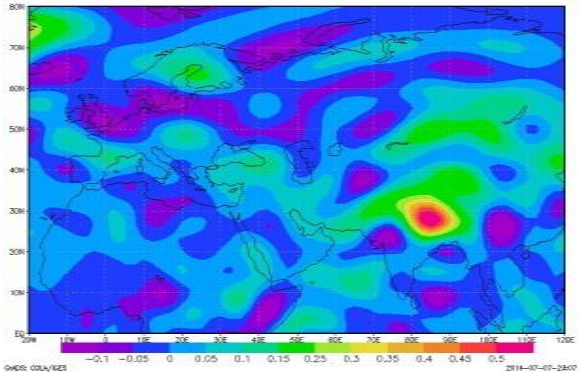

Figure 13 Omega map (1000 hPa) in SLP pattern 3 in dusty days

[DOR: 20.1001.1.23222700.2016.4.4.6.3]

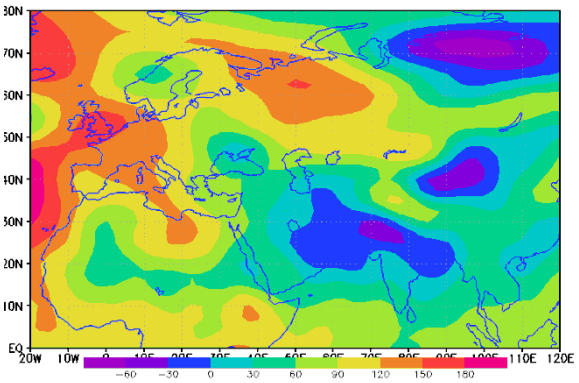

Figure 14 SLP pattern 4 map in dusty days

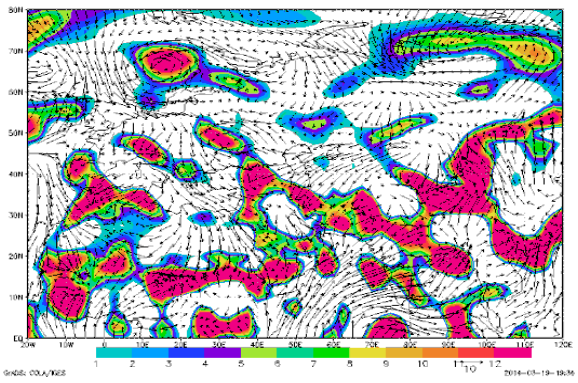

Figure 15 MFC map (1000 hPa) in SLP pattern 4 in dusty days

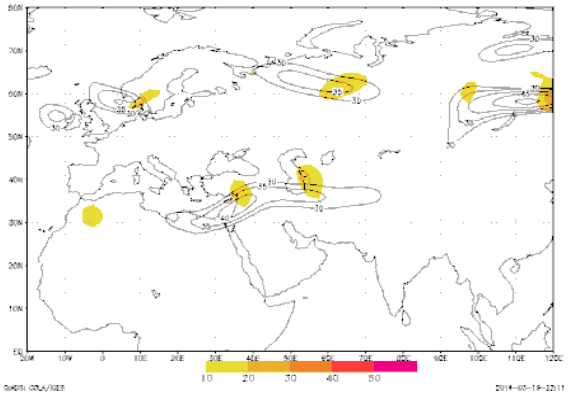

Figure 16 Jet stream map (300 hPa) in SLP pattern 4 in dusty days.

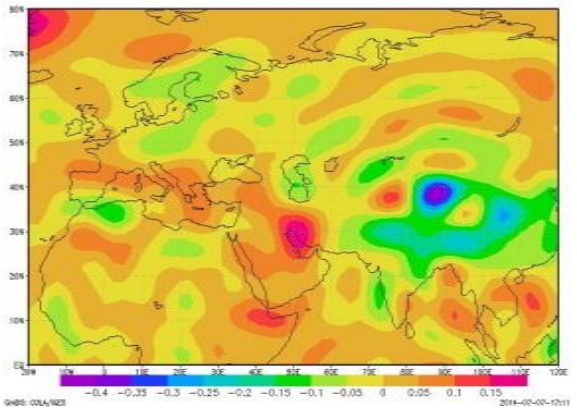

Figure 17 Omega map (1000 hPa) in SLP pattern 4 in dusty days

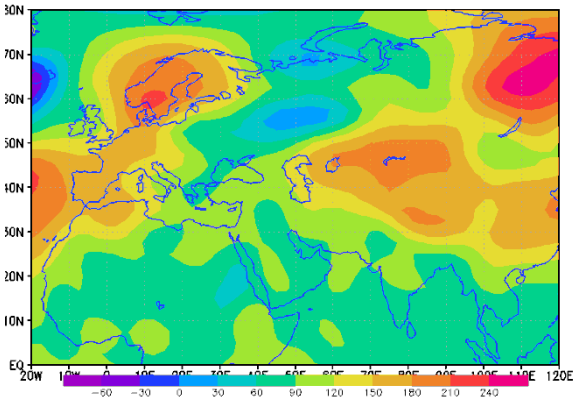

Figure 18 SLP pattern 5 map in dusty days

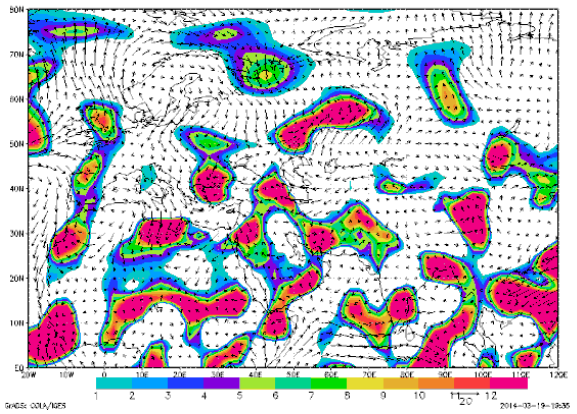

Figure 19 MFC map (1000 hPa) in SLP pattern 5 in dusty days

[DOR: 20.1001.1.23222700.2016.4.4.6.3]

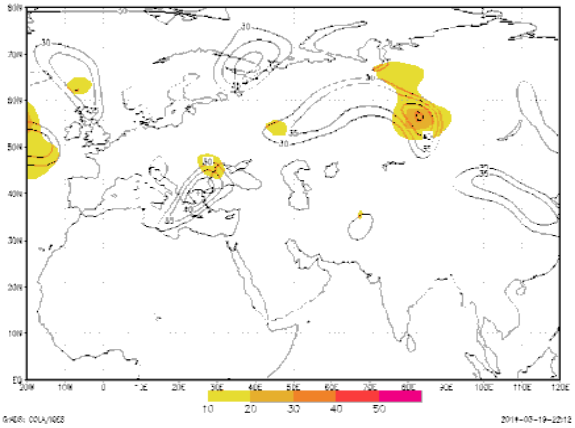

Figure 20 Jet stream map (300 hPa) in SLP pattern 5 in dusty days.

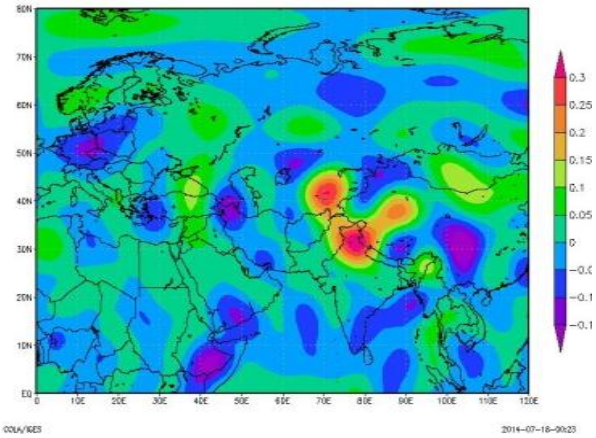

Figure 21 Omega map (1000 hPa) in SLP pattern 5 in dusty days

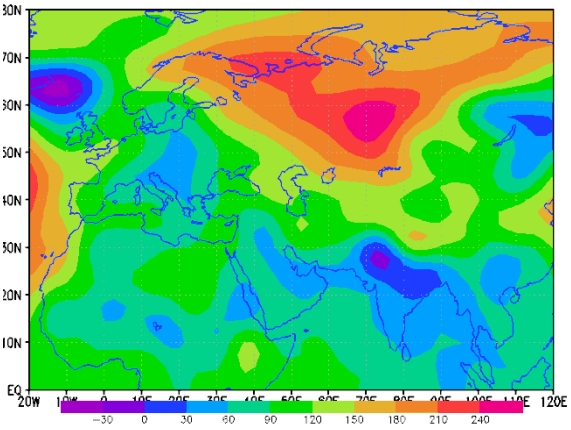

Figure 22 SLP pattern 6 map in dusty days

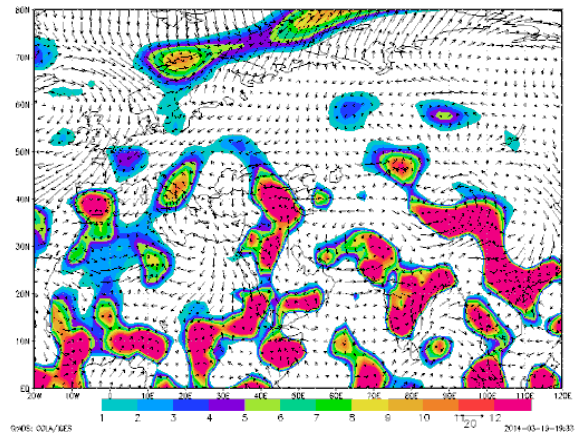

Figure 23 MFC map (1000 hPa) in SLP pattern 6 in dusty days

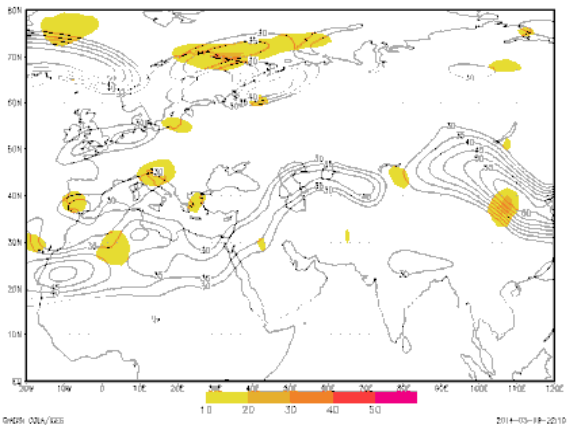

Figure 24 Jet stream map (300 hPa) in SLP pattern 6 in dusty days

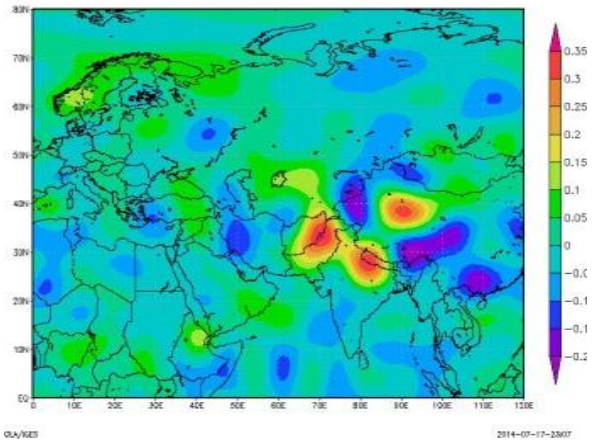

Figure 25 Omega map (1000 hPa) in SLP pattern 6 in dusty days

[DOR: 20.1001.1.23222700.2016.4.4.6.3]

SLP_4 pattern was observed mostly from May to October and the most frequent pattern in May to August; SLP_1 was the only pattern in Jun and July; SLP_3 is the most frequent pattern in March, April and November; SLP_2 was just observed in January. SLP_1 and SLP_3 were the most important circulation patterns in the cold seasons over the Alvand Mountain. SLP_2 pattern was also observed in the cold season, too. SLP_4 was generally the main pattern during the dusty events in the warm season (Figure 26). The Figure 27 illustrates that during the dust events, SLP_4 is the main patterns of the Alvand Mountain that is also observed in all groups. BD_1 dust group was seen in all SLP patterns. BD_2, DIS_2 and BD_3 dust groups have been observed in SLP_3, SLP_4 and SLP_5 patterns. DS_1 dust group was just seen in SLP_4 pattern.

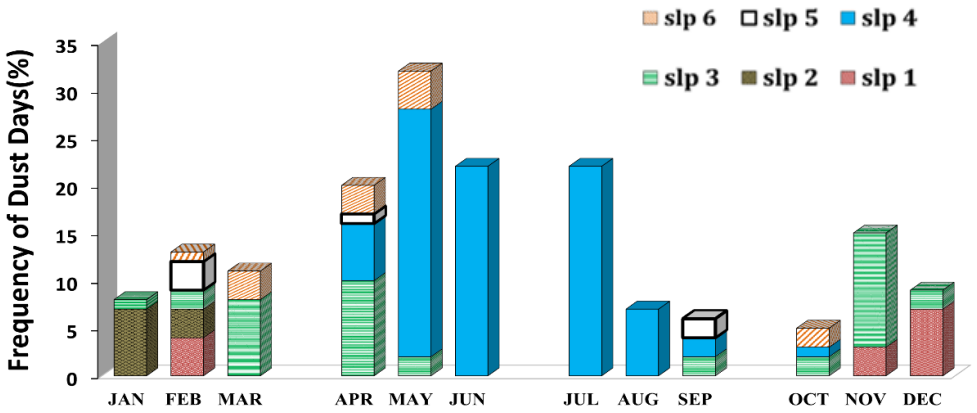

Figure 26 monthly distributions of SLP patterns during the dusty events

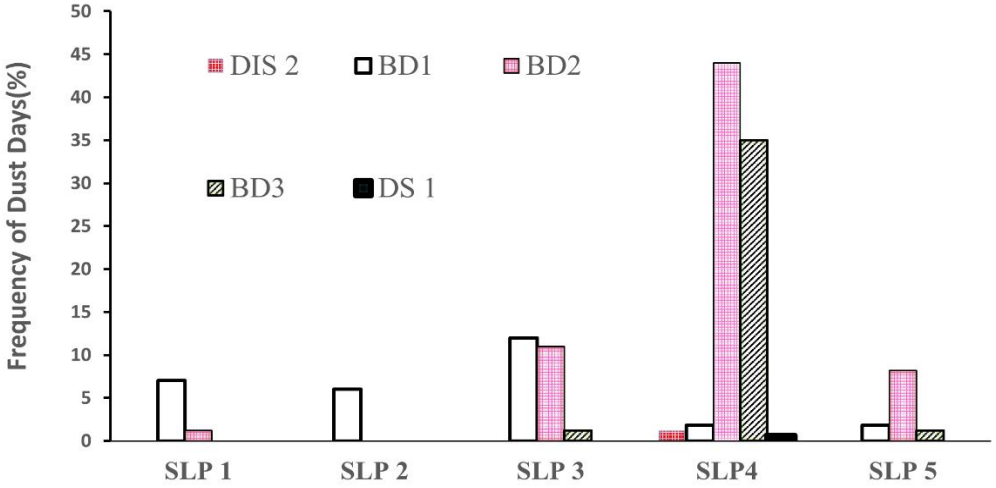

Figure 27 Frequency of circulation patterns in the Alvand Mountain during the dusty events

MFC function in dust groups and pressure patterns are shown in Figure 28. MFC is maximum at 00:00, 12:00 UTC (a, c, e) and significantly decreases at 700, 600 and 500 hPa in different dust groups.

[DOR: 20.1001.1.23222700.2016.4.4.6.3]

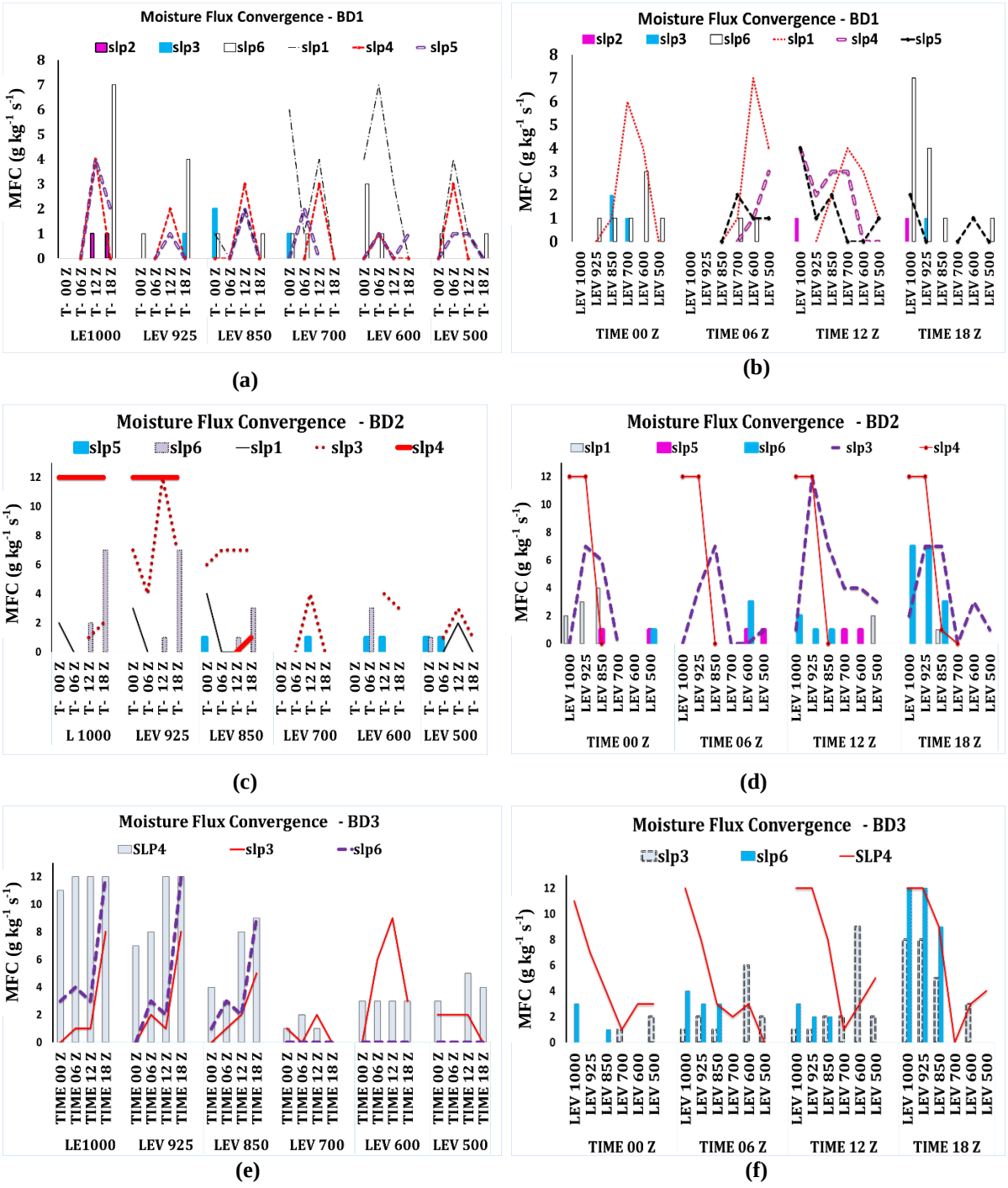

Figure 28 MFC values in dust event categories and SLP patterns over Alvand Mountain

[DOR: 20.1001.1.23222700.2016.4.4.6.3]

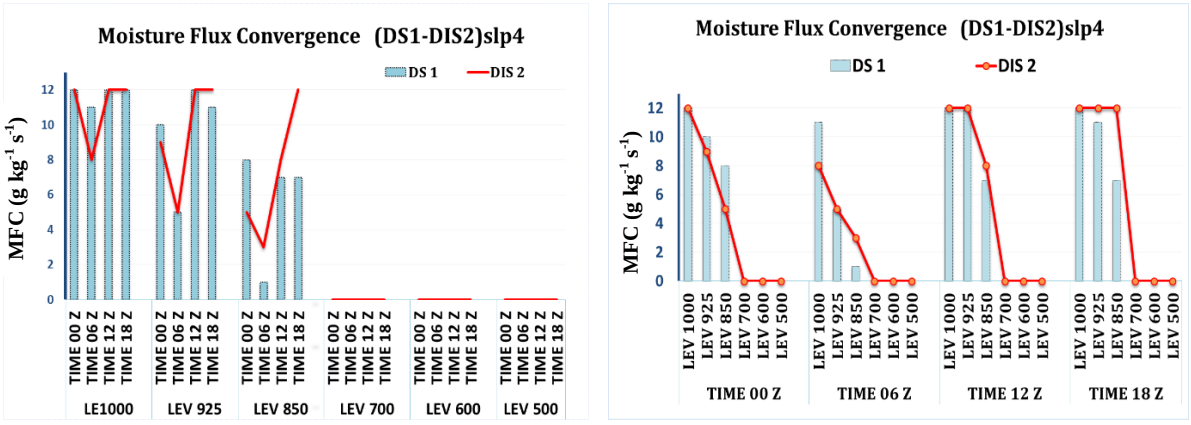

(g) **(h)**

Figure 28 Continued

Values of relative humidity in dust groups and pressure patterns significantly decrease at 12:00 UTC and peaks at 18:00, 00:00 (Figure 29). At different times, SLP3, SLP_5 and SLP_1 patterns have maximum relative humidity in BD_1, BD_2 and BD_3 dusty groups, respectively.

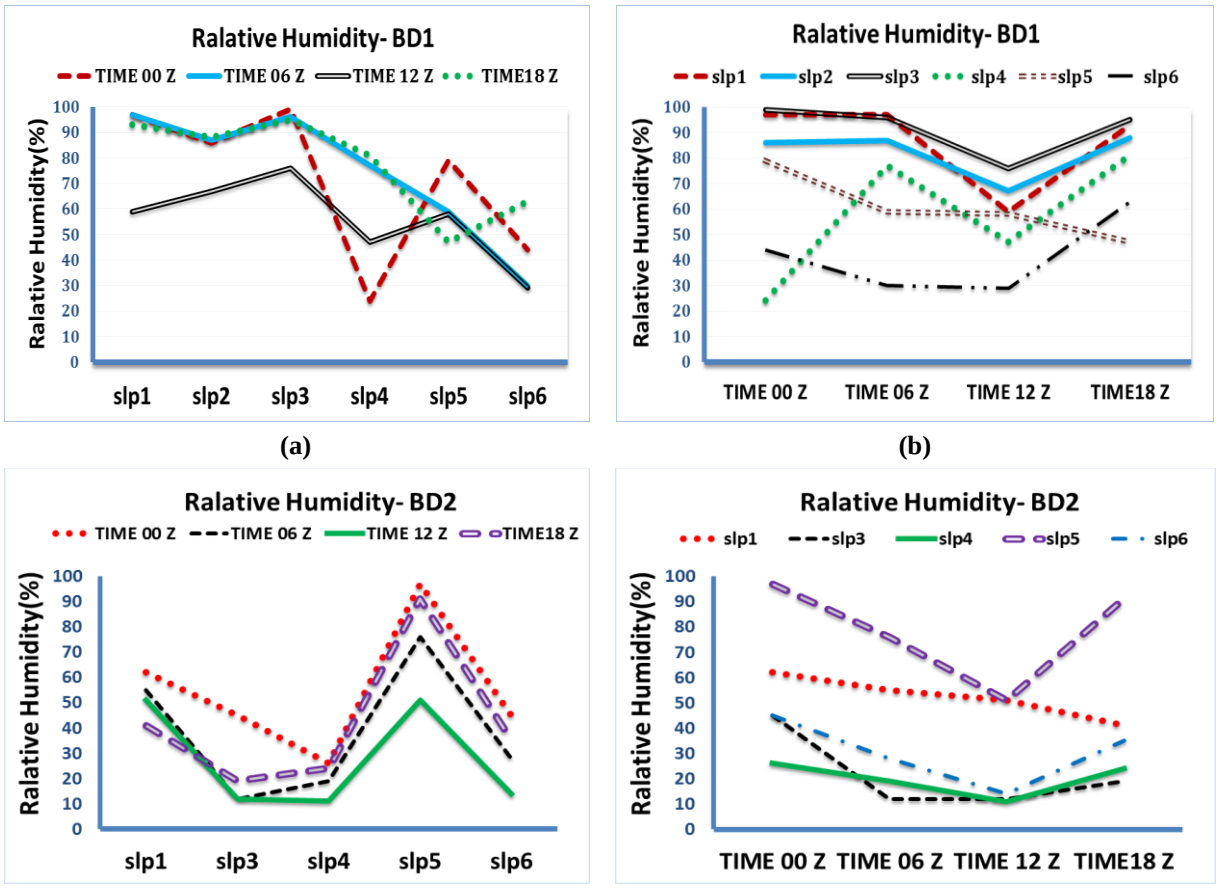

(a) **(b)**

(c) **(d)**

Figure 29 Relative humidity in dusty days at different patterns and times

[DOR: 20.1001.1.23222700.2016.4.4.6.3]

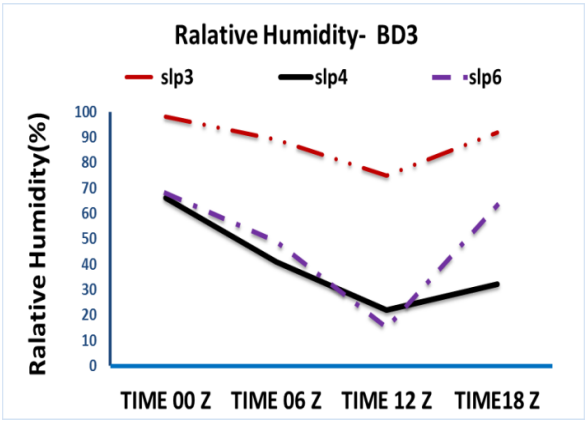

(e)

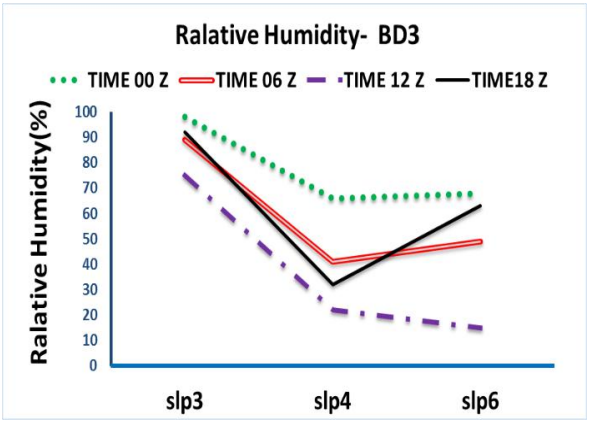

(f)

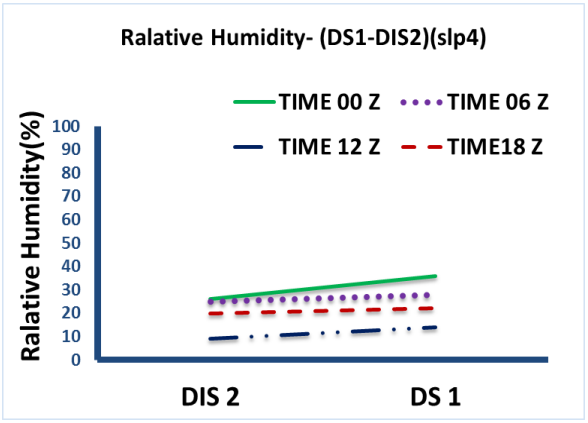

(g)

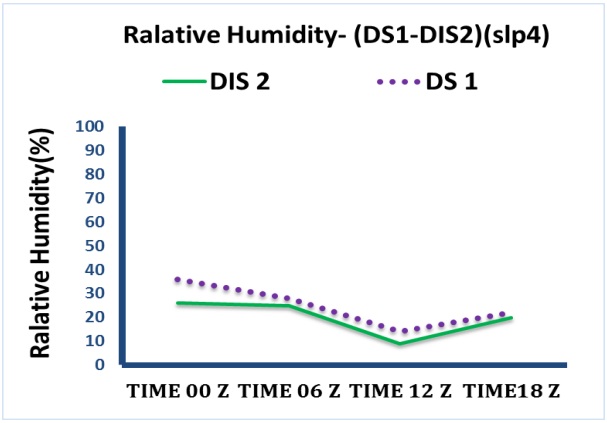

(h)

Figure 29 Continued

4 DISCUSSION AND CONCLUSIONS

The study of the dust groups over the Alvand Mountain adjacent to Hamadan city showed that more than 98 percent of recoded dust phenomenon was "the blowing dust groups (BD) with average intensity", and more than 60 percent of them had outside origin. Dust phenomenon in Hamadan was extensive in all the year, especially in the warm seasons, particularly June. Warm season's dusts are "blowing dust" (BD_2), "dust storm" (DS_1) and "dust-in-suspension" (DIS_2) with outside origin. The important patterns in creation of these groups were SLP_4 and SLP_6 due to the midlevel atmospheric trough and the low-pressure systems of the earth surface, the most important of which were the low-pressure of Persian Gulf and a flow form the east of Turkey and northwest of Iraq with northwestern-southeast directions toward the Persian Gulf, which is the main reason of dust creation and transportation to Hamadan. In this relation, forereach of the cold air accompanies intensive gradient of temperature and pressure on the earth surface and will cause astatic erect flows for creation of dust storms. The cold season's dusts were BD_1 and BD_3 with origins near to the station. The dust groups are caused by SLP_1, SLP_2, SLP_3 and SLP_5 patterns due to high-pressure systems on Iran. Analysis of MFC function in different patterns, levels and times showed a similar conditions in the dust groups during the warm season as moisture convergence function showed the highest value of more than "12 G

[DOR: 20.1001.1.23222700.2016.4.4.6.3]

kg^{-1} S^{-2}" in 1000, 925, 850 hPa, and the lowest value near zero G kg^{-1} S^{-2} in mid-level (700, 600 1nd 500 hPa), especially in the dust-in-suspension (DIS_2) and "dust storm" (DS_1) groups in SLP_4 pattern. During the cold season in the dust groups of BD_2 and BD_1 at lower levels, MFC function was less than 4 G kg^{-1} S^{-2} .Among the dust groups, BD_1 and BD_2 had the least and highest average MFC at different times and levels. BD_2, DIS_2 and BD_3 dust groups have been observed in SLP_3, SLP_4 and SLP_5 patterns. DS_1 dust group was just seen in SLP_4 pattern with a significantly decreased MFC at 12:00 UTC and its maximum value at 18:00, and 00:00. SLP_3, SLP_5 and SLP_3 patterns had maximum relative humidity in BD_1, BD_2 and BD_3 dust groups at different times, respectively. Dust storms generally develop in deserts, but can occur in any area with reduced moisture. Therefore, increase in the relative humidity is supposed to be a practical way to control dust. However, the existence of maximum moisture convergence (12 G Kg^{-1} S^{-2}) was not a dissuasive factor in moving the dust toward the Alvand Mountain and Hamadan. So, the offered strategies such as increasing moisture are inefficient to stop the dust in Hamadan. According to results of Csavina *et al.* (2014), during the dust events in the warm season, there was a high moisture convergence and relative humidity at low levels of atmosphere. This can be attributed to diffusion phenomenon during the occurrence of the dust and the increased density that increased the relative humidity. This process continued up to 27% relative humidity, then decreased with increase in the suspense dusts. Hereon, 06:00 and 18:00 UTC and 700 hap level was recognized as index factors for having the least MFC, creation of sudden changes in the process of moisture convergence, and dynamic conditions of atmospheric patterns in occurrence of dust. So, more studies are required about the effect of 06:00 UTC and 700 hPa level on the dust phenomenon.

5 REFERENCES

Azizi, G., Shamsipur, A. A., Miri, M. and Safarrad, T. Statistical and synoptically analysis of dust in the western half of Iran. Environ. Stud., 2012; 38(63): 123-134.

Banacos, P.C. and Schultz D.M. The use of moisture flux convergence in forecasting convective initiation. Historical and operational perspectives. Weather. Forecast., 2005; 20: 351-366.

Csavina, J., Field, J., Félix, O., Corral-Avitia, A.Y., Eduardo S.A. and Betterton-Eric A. Effect of wind speed and relative humidity on atmospheric dust concentrations in semi-arid climates. Sci. Total Environ., 2014; 487: 82-90.

Farajzadeh-Asl, M., Karimi-Ahmadabad, M., Qaemi, h. and Mobasheri, M.R. The transfer of moisture in winter precipitation in the West of Iran. Modares Journal of Human Sciences, 2009; 13(1): 194-217. (In Persian)

Ghavidel-Rahimi, J. Investigation Moisture Flux Convergence in Super heavy rains of Hurricane Faith over Chabahar coasts. Modares Journal of Human Sciences. 2011; 15: 101-118. (In Persian)

Karimi-Ahmadabad, M., Farajzadeh-Asl, M. Moistures Flux and Spatial and Temporal Patterns of Moistures resources of precipitations in Iran. Geographical Science and Applied Research Journal. 2011; 11(22): 109-128. (In Persian)

Lee, J.J. and Kim C.H. Roles of surface wind, NDVI and snow cover in the recent changes in Asian dust storm occurrence frequency, Atmos. Environ., 2012; 59: 366-375.

[DOR: 20.1001.1.23222700.2016.4.4.6.3]

Mosavi B.M. and Ashraf, B. Study of airs instability and synoptic pattern of dust storms affecting the occurrence of Mashhad. Geography and Regional Development Research Journal. 2012; 18: 27. (In Persian)

Nouri, H., Gayoor, H., Massoodian S.A. and Azadi, M. Investigation of frequency moisture flux convergence and moisture sources precipitation of southern coasts of the Caspian Sea. Geography and Environmental Planning Journal. 2013; 51: 1-14. (In Persian)

Omidvar, K. Synoptic analysis of Sand storms in the desert Yazd-Ardekan. Geographical Research. 2006; 81: 43-87. (In Persian)

Penalba, O., Bettolli, M.L. A classification of the sea level pressure daily fields in southern South America: an application to daily rainfall in the Pampas region. Geophysical Research Abstracts. 2010; Vol. 12, EGU2010-11556.

Saavedra, S., Rodríguez, A., Taboada, J.J., Souto, J.A. and Casares, J.J. Synoptic patterns and air mass transport during ozone episodes in northwestern Liberia. Sci. Total Environ., 2012; 441: 97-110.

United Nations Environment Programme. Establishing a WMO Sand and Dust Storm Warning Advisory and Assessment System Regional Node for West Asia: Current Capabilities and Needs, Technical Report, WMO. 2013; No: 1121.

الگوهای رطوبت نسبی و همگرایی شار رطوبت در زمان رویدادهای گرد و غباری در کوهستان الوند

دیمن غفاری[1*] و حمید نوری[2]

۱- دانش‌آموخته کارشناسی ارشد آبخیزداری، گروه مرتع و آبخیزداری، دانشگاه ملایر، ایران

۲- استادیار آب و هواشناسی، گروه مرتع و آبخیزداری، دانشگاه ملایر، ایران

تاریخ دریافت: ۱۶ آبان ۱۳۹۴ / تاریخ پذیرش: ۲۱ تیر ۱۳۹۵ / تاریخ چاپ: ۱۹ آذر ۱۳۹۵

چکیده فراوانی رطوبت نسبی و شاخص همگرایی شار رطوبت (MFC) در زمان رویداد پدیده گرد و غبار بر فراز کوه الوند بررسی شد. بدین منظور داده‌های دید افقی و رطوبت نسبی در سال‌های ۲۰۰۹-۲۰۱۲ از ایستگاه سینوپتیک همدان و داده‌های سرعت باد و رطوبت ویژه (جهت محاسبه تابع MFC) به همراه فراسنج فشار سطح دریا از سایت NCER /NCAR تهیه گردید. با استفاده از روش ترکیبی تحلیل خوشه‌ای-مولفه‌ی مبنا، گروه‌بندی رویدادهای گرد و غبار و الگوهای هم‌دید انجام شد. سپس تابع MFC برای هر الگوی فشار سطح دریا در سطوح و زمان‌های مختلف محاسبه گردید. نتایج نشان دادند که رویدادهای گرد و غبار و فشار سطح دریا به ترتیب به ۵ گروه و ۶ الگو تفکیک شدند. همچنین بیش‌ترین مقدار شاخص هم‌گرایی شار رطوبت در ترازهای ۱۰۰۰، ۹۲۵ و ۸۵۰ هکتوپاسکال و در ساعت ۱۲:۰۰ و ۱۸:۰۰ UTC محاسبه شد. مقدار MFC در گروه‌های گرد و غبار در سطوح ۷۰۰، ۶۰۰ و ۵۰۰ هکتوپاسکال به شدت کاهش یافت، به‌خصوص در ساعت ۰۶:۰۰ UTC بیش‌ترین میزان کاهش مشاهده شد. بررسی گروه‌های گرد و غبار نشان

[DOR: 20.1001.1.23222700.2016.4.4.6.3]

داد که رطوبت نسبی کاهش قابل توجهی در ساعت ۱۲:۰۰ و بیش‌ترین افزایش را در ساعات ۱۸:۰۰ و ۰۰:۰۰ داشته است.

کلمات کلیدی: امگا، تغییرات زمانی، فشار سطح دریا، طوفان‌های گرد و غبار، همدان

[DOR: 20.1001.1.23222700.2016.4.4.6.3]